JOURNAL OF VIROLOGY, Mar. 2010, p. 2740–2752 Vol. 84, No. 6
0022-538X/10/$12.00 doi:10.1128/JVI.02180-09

Evolution of the HIV-1 *env* Gene in the Rag2$^{-/-}$ $\gamma_C{}^{-/-}$ Humanized Mouse Model$^{\nabla}$

William L. Ince,[1,2] Liguo Zhang,[1,3]† Qi Jiang,[1,3] Kathryn Arrildt,[1,3] Lishan Su,[1,2,3] and Ronald Swanstrom[1,2,3]*

Lineberger Comprehensive Cancer Center,[1] Curriculum in Genetics and Molecular Biology,[2] and Department of Microbiology and Immunology,[3] University of North Carolina, Chapel Hill, North Carolina

Received 14 October 2009/Accepted 16 December 2009

Rag2$^{-/-}$ $\gamma_C{}^{-/-}$ mice transplanted with human hematopoietic stem cells (DKO-hu-HSC mice) mimic aspects of human infection with human immunodeficiency virus type 1 (HIV-1), including sustained viral replication and CD4$^+$ T-cell decline. However, the extent of HIV-1 evolution during long-term infection in these humanized mice, a key feature of the natural infection, has not been assessed fully. In this study, we examined the types of genotypic and phenotypic changes in the viral *env* gene that occur in the viral populations of DKO-hu-HSC mice infected with the CCR5-tropic isolate HIV-1$_{JRCSF}$ for up to 44 weeks. The mean rate of divergence of viral populations in mice was similar to that observed in a cohort of humans during a similar period of infection. Many amino acid substitutions were common across mice, including losses of N-linked glycosylation sites and substitutions in the CD4 binding site and in CD4-induced epitopes, indicating common selective pressures between mice. In addition, *env* variants evolved sensitivity to antibodies directed at V3, suggesting a more open conformation for Env. This phenotypic change was associated with increased CD4 binding efficiency and was attributed to specific amino acid substitutions. In one mouse, *env* variants emerged that exhibited a CXCR4-tropic phenotype. These sequences were compartmentalized in the mesenteric lymph node. In summary, viral populations in these mice exhibited dynamic behavior that included sequence evolution, compartmentalization, and the appearance of distinct phenotypic changes. Thus, humanized mice offer a useful model for studying evolutionary processes of HIV-1 in a complex host environment.

Animal models of HIV-1 infection are important tools for studying transmission, replication, and pathogenesis, as well as therapeutic intervention, of HIV-1 infection. Nonhuman primates such as rhesus macaques, infected with simian or chimeric simian/human immunodeficiency viruses (SIV or SHIV, respectively), represent well-characterized and highly relevant models; however, key limitations include expense, genetic variability of the host animals, and the fact that SIV, while closely related, is distinct from HIV-1. Therefore, small animal models that support HIV-1 infection and recapitulate many aspects of the human infection have been sought using several approaches.

Recent approaches have involved the use of genetically immunodeficient mice that have been reconstituted using human-derived hematopoietic stem cells (HSC) (known as humanized mice). Several models have been developed based on this approach, including Rag2$^{-/-}$ $\gamma_C{}^{-/-}$ (DKO) and NOD/SCID/$\gamma_C{}^{-/-}$ (NOG or NSG) mice transplanted with human HSC (DKO-hu-HSC or NOG-hu-HSC mice) (40, 92) and the NOD/SCID mouse with transplanted human fetal thymus and liver tissue in addition to HSC (62). These models all support HIV-1 infection (1, 3, 6, 30, 87, 96, 102; for a review of these models, see the work of Denton and Garcia [22]). The DKO-hu-HSC mouse lacks both recombination activating gene 2 (Rag2) and the cytokine receptor common gamma chain (γ_C), and as a result, it does not generate murine T, B, and natural killer (NK) cells but supports engraftment of HSC and differentiation of human myeloid and lymphoid lineages. Immune reconstitution in this model likely involves education of human T cells in the mouse thymus and dissemination of differentiated human lymphoid subsets into the peripheral blood and to multiple lymphoid tissues, including lymph nodes, spleen, and bone marrow (92). The DKO-hu-HSC mouse, along with the other humanized mouse models, has been used in studies of transmission (5, 21), pathogenesis (43), and viral inhibition (16, 21, 53, 88, 94).

One important feature of HIV-1 infection is the diversification and evolution of the viral genome over the course of infection. Diversification occurs most prominently in the envelope (*env*) gene, which encodes the viral surface glycoprotein (Env). Env mediates viral entry into cells through attachment to the primary receptor CD4, which primes Env for engagement with a coreceptor, either CCR5 or CXCR4, triggering virion fusion with the cellular plasma membrane (54). HIV-1 infection is typically established by one or a few CCR5-tropic (R5) variants that give rise to an initially homogenous viral population, which then diversifies over the course of chronic infection (45, 84). Diversification of Env results from immune selective pressures (27), isolation in or adaptation to different cellular and anatomical compartments (20, 28, 33, 46, 51), and selection for altered CD4 affinity (72, 90, 95) and coreceptor

* Corresponding author. Mailing address: UNC Center for AIDS Research, CB#7295, Room 22-006, Lineberger Bldg., University of North Carolina at Chapel Hill, Chapel Hill, NC 27599. Phone: (919) 966-5710. Fax: (919) 966-8212. E-mail: risunc@med.unc.edu.

† Present address: Center for Infection and Immunity and National Laboratory of Biomacromolecules, Institute of Biophysics, Chinese Academy of Sciences, 15 Datun Road, Chaoyang District, Beijing 100101, China.

$^{\nabla}$ Published ahead of print on 30 December 2009.

tropism (26, 39). In many cases, during late-stage infection, variants emerge from the R5 virus population that are CXCR4 tropic (X4), an event that is often associated with accelerated CD4 T-cell loss and progression to AIDS (9, 18, 89). In an effort to determine if any of these aspects of HIV-1 evolution are exhibited in the humanized mouse model, we examined the extent of HIV-1 diversification and the types of evolutionary changes that occur in *env* in mice infected with CCR5-tropic HIV-1 for up to 44 weeks.

Sampling of viral *env* variants from the peripheral blood plasma over the course of the infection revealed increasing diversity and divergence of the viral population at rates similar to those observed in natural infection. Mutations were identified that affected Env conformation and sensitivity to neutralizing antibodies, CXCR4 coreceptor use, and potential N-linked glycosylation sites. Other mutations potentially affecting the Env phenotype were identified in CD4 binding sites and CD4-induced epitopes. The patterns of substitutions indicated that certain sites were under selection, particularly in cases where the same substitution was identified in multiple mice.

This study demonstrates the potential for studying HIV-1 evolution in the DKO-hu-HSC mouse model and also gives insight into the types of selective pressures driving HIV-1 *env* evolution in this host environment. These findings, while highlighting some of the limitations of this model, will help to inform its appropriate use for studying different aspects of HIV-1 infection, such as the evolutionary constraints placed on HIV-1 during natural infection and in the face of pharmacological and immunological inhibition.

MATERIALS AND METHODS

Model generation. $Rag2^{-/-}$ $\gamma_C{}^{-/-}$ immunodeficient newborn mice were injected intrahepatically with human $CD34^+$ hematopoietic stem cells. Two separate $CD34^+$ cell donors were used to reconstitute mice 5 to 8 and mice 64 and 67 (donors A and B, respectively, in Table 1). After 8 to 12 weeks, immune system reconstitution was confirmed. HIV-1_{JRCSF} (GenBank accession number M38429.1) was generated by transfection of 293T cells with an infectious clone expression plasmid, pYK-JRCSF (52), obtained from the National Institutes of Health AIDS Research and Reference Reagent Program (ARRRP). Cell-free supernatant was used to intravenously infect reconstituted mice. Five mice from cohort A (mice 4 to 8) and four mice from cohort B (mice 63 to 67) were infected. Mice from each cohort that were successfully engrafted, successfully infected, and kept alive with active infection for at least 22 weeks were analyzed. Viral load was monitored for 44 weeks in mice 5 to 8 and for 22 weeks for mice 64 and 67.

As part of an additional study investigating the role of $CD4^+$ $CD25^+$ $Foxp3^+$ T regulatory cells (Treg cells) in HIV-1 infection, mice 6 to 8 were treated at 43 weeks postinfection with denileukin diftitox (also called DAB_{389}IL-2 or Ontak), which selectively depletes Treg cells (43, 55). Treg cells account for 1 to 4% of all $CD4^+$ T cells in this model, and Ontak treatment usually results in selective depletion of Treg cells, by as much as 90% (43). Treatment with Ontak correlated with increased immune activation, as measured by CD38 expression, and Ontak-treated mice also exhibited a greater percentage of infected cells and greater $CD4^+$ T-cell depletion. Ontak treatment may have increased viral replication, perhaps as an effect of global enhancement of $CD4^+$ T-cell activation. While there were unique evolutionary events observed in individual mice, there was no clear distinction in the patterns of viral evolution between treated and untreated animals.

Sample collection. Mice were monitored for peripheral blood viral loads and CD4/CD8 ratios for up to 44 weeks. Peripheral blood samples (~30 μl) were collected at 3, 10, 22, 40, and 44 weeks postinfection. Mice were sacrificed and tissue was harvested at 22 weeks (mice 64 and 67) and 44 weeks (mice 5 to 8) postinfection.

Nucleic acid extraction. Viral RNA was extracted from the available volume of blood plasma (~30 μl) by use of a QiaAmp viral RNA kit (Qiagen, Valencia, CA) and was eluted in 60 μl distilled water. Total DNA was extracted from tissue, using a PicoPure DNA extraction kit (Molecular Devices, Sunnyvale, CA). Pelleted cells extracted from collagenase-treated tissue (about 10^5 to 10^6 cells) were resuspended in 50 μl of PicoPure buffer containing proteinase K. The extraction suspension was incubated at 65°C for 8 h and used directly for PCRs as described below.

Viral RNA and DNA amplification and sequencing. The 60-μl RNA eluate was reverse transcribed using the Superscript III reverse transcriptase (RT) system (Invitrogen, Carlsbad, CA) and an oligo(dT) primer. A region of the HIV-1 genome encompassing *env* through the 3′ U3 region was amplified from cDNA by a limiting-dilution PCR approach (single-genome amplification [SGA]) initially described by Simmonds et al. (86) and Edmonson and Mullins (24) and then modified by Palmer et al. (70) and Salazar-Gonzalez et al. (80). Primers and thermocycling procedures for amplification and sequencing were used as previously described by Keele et al. (45) but were modified by replacing the downstream *env* amplification primer set with a primer that captures the U3 region, with the sequence 5′-AAGCACTCAAGGCAAGCTTTATTG-3′. The same procedure used for amplifying cDNA was used to amplify the envelope gene from viral DNAs extracted from tissue samples. Automated sequencing followed by manual editing of sequences was carried out on SGA amplicons, using the Big Dye Terminator system (Applied Biosystems, Foster City, CA).

HIV-1 sequencing data from human infections. HIV-1 sequences from human infections were obtained from the work of Shankarappa et al. (84) and Salazar-Gonzales et al. (81).

Sequence analysis. Subtype B sequences used for assessment of sequence conservation at specific sites were accessed through the Los Alamos National Laboratories HIV Sequence Database (http://www.hiv.lanl.gov). Sequence alignments were generated using MAFFT (multiple alignment using fast Fourier transform) (44). The best-fitting substitution rate model for each alignment was determined using FindModel, a variation of Modeltest (75), implemented through http://www.hiv.lanl.gov/content/sequence/findmodel/findmodel.html. Maximum likelihood (ML) phylogenies were generated in PhyML, using the best-fitting model (GTR or HKY85 in this study), four rate substitution categories, and the PhyML-determined gamma shape parameter and number of invariant sites. Potential N-linked glycosylation (PNLG) sites were identified using N-Glycosite (103), implemented through http://www.hiv.lanl.gov/content/sequence/GLYCOSITE/glycosite.html. Divergence was determined as the mean genetic distance of sequences to the founder sequence at a given time point. In the case of mouse viral populations, the founder sequence was that of HIV-1_{JRCSF}, and in the case of human viral populations, the "founder" sequence was taken to be the consensus of sequences sampled at 2 to 5 months postseroconversion for the Shankarappa et al. sequence set and an estimated 20 to 24 days postinfection for the Salazar-Gonzales et al. sequence set. Distances were determined from ML tree branch lengths by use of Branchlength, implemented through http://www.hiv.lanl.gov/content/sequence/BRANCHLENGTH/branchlength.html.

Selection analysis was carried out by determining the rates of synonymous and nonsynonymous substitutions (67, 69). Rates were determined using SNAP (50), as implemented through http://www.hiv.lanl.gov/content/sequence/SNAP/SNAP.html. A Wilcoxon signed rank test was used to compare rates of synonymous and nonsynonymous base substitutions within mouse populations.

Linkage disequilibrium analysis was performed using DNAsp v5 (58). Fisher's exact test was used to determine the significance of nonsynonymous nucleotide substitution associations.

Env phenotype assays. *env* gene expression vectors were generated from selected amplicons by use of a pcDNA3.1 Directional TOPO expression kit (Invitrogen, Carlsbad, CA). 293T cells were cotransfected with *env* expression vectors and the pNL4-3.Luc.R−E− luciferase reporter vector (34) (obtained from ARRRP), using the Fugene transfection reagent (Roche, Mannheim, Germany) according to the manufacturer's protocol, to generate pseudovirus. Cells were washed with phosphate-buffered saline 8 to 12 h after transfection in order to reduce transfection complex carryover and background luciferase expression in target cells, which was monitored with an Env-negative control. Virus supernatant was collected 48 h after transfection. The coreceptor phenotype was determined based on detection of luciferase activity in U87.$CD4^+$ cells expressing either CCR5 or CXCR4 (8) (obtained from ARRRP), using a luciferase assay system kit (Promega, Madison, WI). Pseudovirus was incubated with U87.CD4.CXCR4/CCR5 cells for 36 to 48 h prior to lysis of cells and measurement of luciferase activity. Coreceptor-dependent viral entry was confirmed using inhibitory concentrations of AMD3100 (35) (CXCR4 inhibitor) or TAK-779 (2) (CCR5 inhibitor) (both obtained from ARRRP). Sensitivity to neutralization by the anti-V3 antibodies 447-52D (17) (ARRRP) and 19b (11) (a gift

TABLE 1. Immune reconstitution and CD4$^+$ T-cell depletion

Mouse no.	HSC donor[a]	% hCD45$^+$ cells in peripheral blood[b]	CD4/CD8 ratio	
			Preinfection[c]	At termination[d]
5	A	9.3	14.69	6.833
6	A	15.1	6.67	0.579
7	A	7.9	4.18	0.317
8	A	15.9	10.91	0.006
64	B	23.7	1.35	0.039
67	B	9.8	1.51	0.263

[a] Mice were reconstituted with one of two CD34$^+$ HSC donors, A and B.
[b] Percentage of cells expressing human CD45 (hCD45) in the peripheral blood, determined 11.5 weeks after hCD34$^+$ cell transplantation.
[c] The harmonic mean ratio of CD4$^+$ to CD8$^+$ T cells in the peripheral blood for 2 samplings prior to infection.
[d] Ratio of CD4$^+$ to CD8$^+$ T cells in the peripheral blood at termination, i.e., at 44 weeks for mice 5 to 8 and 22 weeks for mice 64 and 67.

from James E. Robinson) was assessed on TZM-BL cells (obtained from ARRRP), which are permissive to X4 and R5 viruses and contain an integrated, Tat-responsive luciferase cassette (72). Sensitivity to the anti-CD4 antibody Leu3a (CD4 Pure) (BD Biosciences, San Jose, CA) was assessed on U87.CD4.CCR5 cells.

Viral fusion kinetics were measured on U87.CD4.CCR5 cells in a 96-well format in triplicate. Pseudotyped virus supernatant and cells were cooled to 4°C and spin inoculated (spinoculated) for 2 h at this temperature to synchronize entry. Immediately after spinoculation, the medium was removed from cells and replaced with medium prewarmed to 37°C. The fusion inhibitor T20 (obtained from ARRRP) was added at the inhibitory concentration of 200 nM at time zero for the first well and at 5-min intervals for successive wells, for up to 70 min. The time to one-half maximal entry was used to compare viruses.

Nucleotide sequence accession numbers. The GenBank sequence accession numbers for sequences generated in this study are GQ412353 to GQ412705.

RESULTS

Diversification and divergence of HIV-1$_{JRCSF}$ over the course of infection in a mouse model with sustained viral infection. Six DKO-hu-HSC mice with stable human leukocyte reconstitution were infected intravenously with HIV-1$_{JRCSF}$, a CCR5-tropic isolate of HIV-1 generated from an infectious molecular clone. Viral infection persisted in all mice over the period of observation: 44 weeks for mice 5, 6, 7, and 8 and 22 weeks for mice 64 and 67, which received HSC from a different donor (Table 1). The viral RNA load in the blood exhibited a slow decay of about 1 $\log_{10}$ over the course of 44 weeks in mice 5 to 8 (Fig. 1), consistent with other reports using this model and different HIV-1 isolates (3), although the reason for this drop is not known. A relative decline in CD4 T cells was also observed (Table 1).

Given that these mice were able to support infection for 22 to 44 weeks, we wanted to know if and to what extent the viral population had diversified, as is observed in human infections over a similar period. Viral RNA was extracted from the peripheral blood plasma and subjected to SGA of the entire *env* gene, a limiting-dilution RT-PCR technique designed to facilitate direct sampling of viral genomes and to avoid PCR-generated mutations and recombination. Sequence diversification and divergence of HIV-1$_{JRCSF}$ in the peripheral blood were assessed for a region of *env* that encodes variable loops 1 through 5 (V1 to V5) of gp120, at the following time points: weeks 10, 40, and 44 postinfection for mice 5 and 6; weeks 3, 40, and 44 for mouse 8; and weeks 4 and 22 for mice 64 and 67. The median number of sequences sampled at each time point was 16.5, and the numbers ranged from 11 to 39 sequences.

A maximum likelihood phylogeny of sequences from the last time point (week 22 for mice 64 and 67 and week 44 for mice 5 to 8) for each mouse is presented in Fig. 2. Sequences were generally clustered by mouse, indicating distinct evolutionary paths that could distinguish mouse viral populations.

For a region of *env* encompassing C2 to V5, the rate of divergence from the founder virus in the mice was compared to that observed in two data sets for infected humans sampled either prior to seroconversion and at time points 3 to 19 months later (Salazar-Gonzales et al. [81]) or after seroconversion and at time points 9 to 24 months later (Shankarappa et al. [84]). In the former study, viral populations from three subjects were initially sampled prior to seroconversion, at an estimated 20 to 24 days postinfection and 9 to 16 days prior to seroconversion. In the latter study, viral populations from 7 subjects were initially sampled within 2 to 5 months after seroconversion. In both data sets, the viral populations at the first time points sampled were relatively homogeneous, and these populations were compared to those present at the later time points. Divergence was determined as the mean distance (branch length) of sequences in a population at a given time point from the "founder" virus sequence, which was either the consensus of sequences sampled at the first time point for the human infections or HIV-1$_{JRCSF}$ (GenBank accession number M38429.1) for the mouse infections. The rate of divergence was calculated by using the mean divergence from the founder of a population at the last time point measured divided by the time postinfection. The mean rates of divergence in mice and in the postseroconversion human data sets were 0.0175%/week (range = 0.034 to 0.0043%/week) and 0.018%/week (range = 0.007 to 0.030%/week), respectively, which were statistically indistinguishable ($P = 0.96$) (Fig. 3A). The mean rate of divergence in the pre-to-postseroconversion data set was also similar (0.015%/week; range = 0.004 to 0.026%/week; $P = 0.706$), although slightly lower than that observed in mice. The mean level of diversity (Fig. 3B) in viral populations in humans, extrapolated to 44 weeks, was greater than but still not statistically different from that observed in mice ($P = 1$ for comparison to the pre-to-postseroconversion human data set and $P = 0.5338$ for comparison to the post-

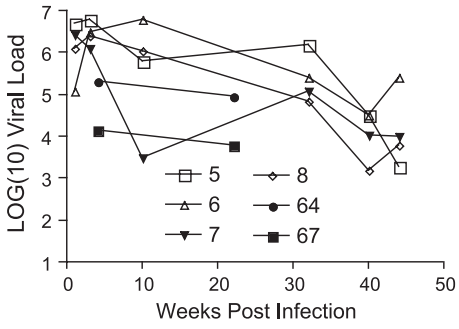

FIG. 1. Plasma viral loads over 44 weeks of infection for mice 5 to 8. The DKO-hu-HSC mice were infected intravenously with HIV-1$_{JRCSF}$. HIV-1 viremia in plasma samples (copies/ml) from all infected DKO-hu-HSC mice were measured at 3, 10, 22, 40, and 44 weeks postinfection for mice 5 to 8 and at 4 and 22 weeks postinfection for mice 64 and 67.

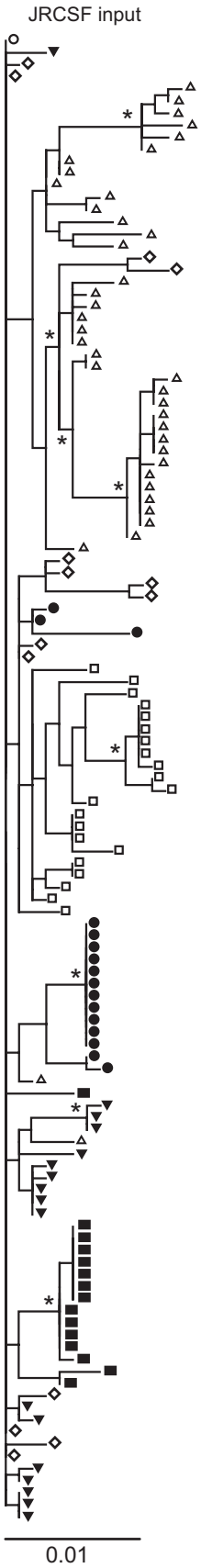

seroconversion data set). The rates of divergence and diversification of HIV-1 in mice fell within the distribution of the rates measured in the two different human cohorts sampled starting at different points around the time of seroconversion. These similarities are in spite of the likely absence of an HIV-1-specific antibody response in the mouse, which is low to undetectable in this model throughout infection, a selective pressure that plays a major role in Env divergence and diversification in human infection postseroconversion (27). In this regard, Western blot analyses of plasmas from the mice used in this study, taken early and late after infection, were uniformly negative for reactivity to HIV-1 antigens (data not shown). We conclude that there is no major difference in the evolutionary rate of HIV-1 within *env* in this mouse model over the first 44 weeks from the time of infection from that for an analogous early stage of human infection, although the selective pressures in these two settings likely differ (see below).

Features of *env* sequence evolution in mice. We next wanted to examine the types and patterns of nucleotide substitutions that contribute to diversity. One distinctive mechanism that may contribute to sequence diversity during natural infection is the activity of the antiviral factor APOBEC3G (A3G) (42), which can give rise to disproportionate numbers of G-to-A transitions in the plus-strand sequence in natural infection, in spite of the A3G antagonist activity of the viral Vif protein, indicating hypermutation of the nascent minus-strand DNA by A3G (59, 78, 101). Examining *env* sequences from mice revealed a subset (1 to 4%) of hypermutated sequences exhibiting a disproportionate number of G-to-A transitions in A3G target motifs in each mouse, indicating that this mechanism is at work in this model. This observation also suggests that A3G may contribute some proportion of G-A transitions observed at A3G recognition sites in sequences that are not overtly hypermutated.

A key feature of this model is the isogenicity of hosts reconstituted with the same donor. We were interested to see if any common amino acid substitution patterns emerged in different mice. Common amino acid substitutions represented in viral populations of multiple mice likely represent selected changes rather than mutations that occurred via genetic drift, as might be the case for substitutions represented in only one mouse.

Substitutions that grew out (i.e., were seen in more than one sequence either within or between mice) in each mouse viral population are depicted in Fig. 4 and are categorized by their potential functional effects, along with the numbers of mice in which they were detected. Within a 380-amino-acid region encompassing V1 through V5 and much of conserved region 5 (C5), substitutions at a total of 45 positions grew out. These mutations were concentrated in the variable loop regions of

FIG. 2. Phylogeny of HIV-1 sequences from all mice. The tree is a maximum likelihood tree of V1-to-C5 sequences from the peripheral blood at week 44 for mice 5 to 8 and at week 22 for mice 64 and 67. Symbols at branch tips indicate the mouse number. Open square, mouse 5; open triangle, mouse 6; closed triangle, mouse 7; diamond, mouse 8; closed circle, mouse 64; closed square, mouse 67. The open circle at the top of the tree indicates the JRCSF input sequence. Asterisks indicate bootstrap values of >70%. The scale bar indicates the number of substitutions per site.

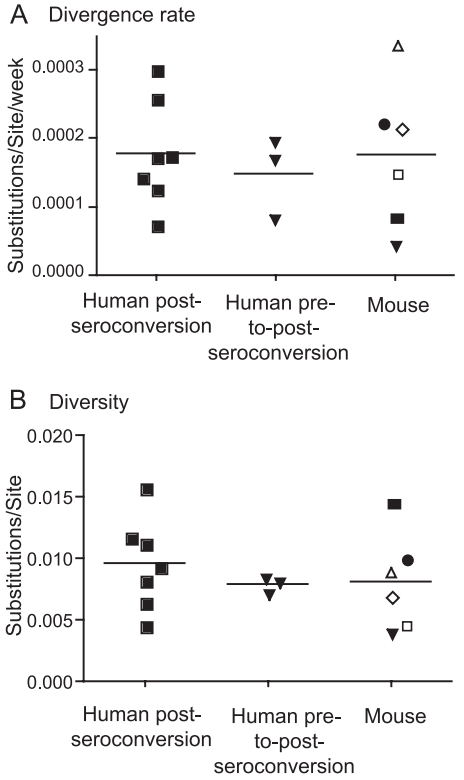

FIG. 3. Comparison of divergence rates and diversity levels in mice and humans. Distance measurements were based on branch lengths of maximum likelihood trees. Symbols for the mouse group in panels A and B indicate the mouse number. Open square, mouse 5; open triangle, mouse 6; closed triangle, mouse 7; diamond, mouse 8; closed circle, mouse 64; closed square, mouse 67. (A) Divergence rates in mice and in human cohorts initially sampled postseroconversion (human postseroconversion) (86) and preseroconversion (human pre-to-postseroconversion) (83) were measured for the C2-to-V5 region of *env*. For the postseroconversion data set, the mean distance, based on branch lengths of a maximum likelihood tree, was measured from the consensus at a time point 2 to 5 months postseroconversion for variants sampled at time points 9 to 24 months later. Sequences sampled at the first time point were relatively homogeneous, except for two subjects who were likely infected with two variants and were removed from the analysis. For the pre-to-postseroconversion data set, mean distance was measured from the consensus at time points estimated to be 20 to 24 days postinfection and 9 to 16 days prior to seroconversion for variants sampled 3 to 19 months later. Mean distance was divided by the time between sampling points to obtain the rate of divergence. For mice, the mean distance was measured from HIV-1_{JRCSF} for variants sampled at the last time point, at either 22 or 44 weeks postinfection. (B) Population diversity is represented as the mean pairwise distances within populations at or extrapolated to 44 weeks postinfection, for mouse and pre-to-postseroconversion human samples, or postseroconversion for the postseroconversion human samples. The student *t* test was used to determine *P* values for differences between distributions. *P* values for all comparisons were >0.2.

Env ($P = 0.0001$; Fisher's exact test). However, no insertions or deletions were observed. Of the substitutions that grew out in mouse viral populations, 19 were detected in more than one mouse, and each of the 4 substitutions that were detected in three or more mice (D167N, N386K/S, N411D/S, and E482K) were represented in both donor sets (Fig. 4).

Evidence of positive selection can also be obtained by determining the ratio of nonsynonymous to synonymous base substitution rates (dN/dS). Ratios of >1 and <1 indicate positive and negative selection, respectively. For the *env* region encompassing V1 to C5, the dN/dS ratio was >1 for viral populations in mice 6 (1.48) and 8 (1.32), which also showed the highest levels of divergence (Fig. 3), nearly 1 in mouse 67 (1.03), and <1 in mice 5 (0.79), 7 (0.82), and 64 (0.57), although the differences between rates of synonymous and nonsynonymous mutations were significant only for mice 6 ($P = 0.0126$; dN/dS = 1.48) and 64 ($P = 0.0001$; dN/dS = 0.57). We interpret these results with caution, because this analysis is limited in its sensitivity when there are too few substitutions to provide statistical power or when only a few sites are under positive selection, which is often the case in Env early in infection.

Substitutions identified at multiple potential N-linked glycosylation sites. Glycosylation of Env at numerous sites has been shown to play a role in proper protein folding, receptor and coreceptor engagement (57, 73), and escape from neutralizing antibodies (15, 47, 97). We identified one substitution, S142N in mouse 6, that added a PNLG sequon [$NX_1(S/T)X_2$, where X represents any amino acid other than proline (29)] in V1 and adjacent to a preexisting PNLG site in HIV-1_{JRCSF}, which remained intact (Fig. 4). In contrast, substitutions that disrupted PNLG sequons were observed at seven positions and included the following (mean frequencies are indicated in parentheses): N160K (8%), N187D (36%), N230S (43%), N241D (5%), N339K/D (8%), N386K/S (86%), N411D/S (40%), and T413I (36%) (Fig. 4). All substitutions, except N160K and N241D, were detected by week 10. Substitutions N339K/D, N386K/S, N411D/S, and T413I were identified in more than one mouse, suggesting that the loss of glycosylation at these sites was under some level of selection, although the low frequency of the N339K/D substitution, at no more than 12%, suggests that selection at this site was weak. The N386K/S substitution, which rose to the highest frequency in the three mice in which it was detected (mean, 86%), and the N339K/D substitution are located in the V4 and C3 regions, respectively, and are part of the neutralizing antibody 2G12 epitope. Loss of these PNLG sites individually and in combination has been shown to confer resistance to this antibody (60, 93). The PNLG sequon composed of N411 and T413, located in V4, has been shown to covary with a number of other PNLG sequons and likely plays a role in the glycosylation of Env as a means of antibody escape (74, 97). The net loss of PNLG sites was widely distributed across Env, indicating that the heavy glycosylation of Env observed in natural infection may not be required for viral persistence in this model and may reflect the lack of a strong humoral immune response; maintenance of these glycosylation sites likely has a fitness cost for replication.

HIV-1_{JRCSF} evolves to become sensitive to specific anti-V3 antibodies. Previous studies using the DKO-hu-HSC model have found the humoral immune response to HIV-1 to be weak (3) or undetectable (1, 30, 102), and we did not detect any HIV-specific antibodies in the mice in this study. Primary isolates of HIV-1 passaged in cell culture in the absence of neutralizing antibody pressure evolve to become sensitive to a spectrum of heterologous neutralizing antibodies (4, 65, 99). The antibody 447-52D is specific for a conserved epitope at the tip of the Env V3 loop and neutralizes viral isolates that are

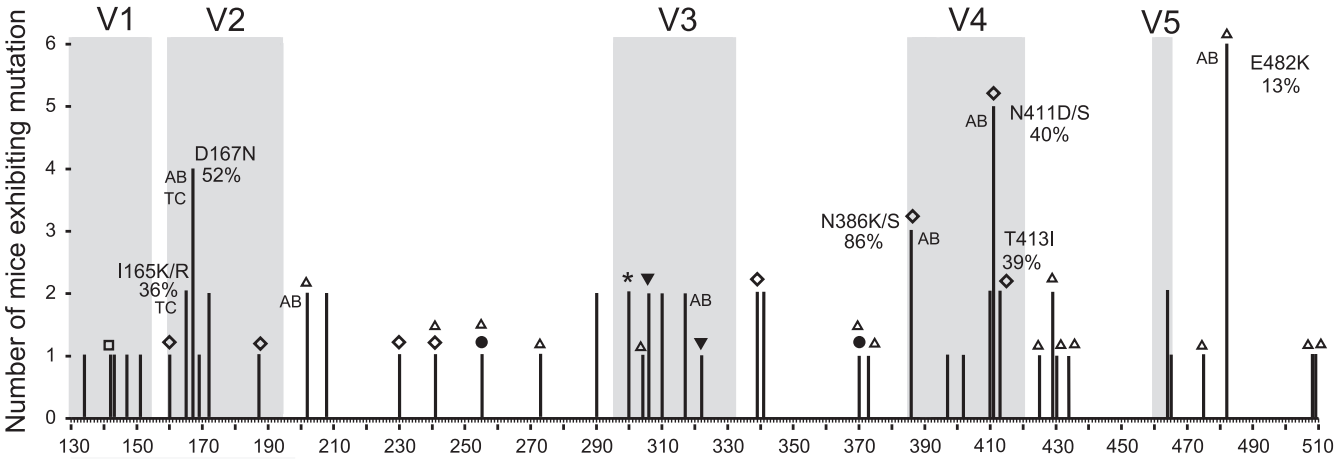

FIG. 4. Positions and classifications of amino acid substitutions in the V1-to-C5 region of Env. Amino acid numbering on the abscissa corresponds to the HXB2 reference sequence. Bars on the graph indicate positions of substitutions and the frequency with which substitutions were identified in a mouse population at the final time point postinfection. Variable loops are shaded in gray. Substitution types are indicated by symbols. Square, addition of a PNLG site; diamond, loss of PNLG site; open triangle, >95% sequence conservation in subtype B; closed circle, component of the CD4 binding domain; asterisk, reversion to subtype B consensus; closed triangle, linked to coreceptor tropism. Substitutions at positions 165 and 167 that affected Env conformation and substitutions identified in three or more mice are indicated along with their mean percent abundances in the population. Substitutions identified in both donor sets are indicated by "AB" (see Table 1). "TC" indicates substitutions associated with tissue culture adaptation in other studies (see Discussion). Assessment of >95% sequence conservation was based on a random sampling of 300 sequences (one per patient) from the Los Alamos HIV Sequence Database. Sequencing of 30 SGA amplicons from the inoculum revealed four single point mutations among three amplicons. One of these mutations, at codon 151, was observed later in infection, in mouse 67.

known to have a history of cell culture passage, while primary isolates can encode the epitope but remain largely resistant (7, 17, 83). Sensitivity of cell culture-passaged virus to this and other V3 antibodies, such as 19b, is attributed to a loss of the Env conformation that masks the V3 epitope (61, 100). We were therefore interested in assessing the extent to which HIV-1_{JRCSF}, which encodes the V3 epitopes but is resistant to 447-52D, had evolved sensitivity to this antibody. *env* clones that included a broad spectrum of substitutions were generated from the amplicons from five mouse viral populations at the last time point (week 44 for mice 5 to 8 and week 22 for mouse 64). Screening of the *env* clones generated from these mice for expression of an Env protein with sensitivity to 447-52D (as tested in a pseudovirus assay) revealed a subset of clones in four of the five mice that encoded Env proteins that were neutralization sensitive compared to the input virus Env (Fig. 5A). Two mutually exclusive mutations, N165R/K and D167N, near the base of the V2 loop, appeared to be linked to neutralization sensitivity, as one or the other was present in all neutralization-sensitive Envs and absent in those that remained resistant (Fig. 5A and B). These mutations were detected early in infection. The D167N mutation was detected at week 10 in mice 5 and 6, and both N165K/R and D167N mutations were present in mice 5 and 6 at week 44. Mice 8 and 64 exhibited only the D167N mutation, which was detected in these mice at 22 and 44 weeks postinfection, respectively. The frequencies of these mutations in a population were, on average, 36% and 52% for N165R/K and D167N, respectively. Neither mutation was detected in mouse 7 or 67. When these mutations were reintroduced into HIV-1_{JRCSF} *env* individually, they rendered the virus relatively neutralization sensitive (Fig. 5C). We also tested these mutants, along with several of the 447-52D-sensitive clones, for sensitivity to another V3-specific antibody, 19b, and obtained similar results (data not shown). The frequency with which these substitutions were detected suggests that viruses replicating in these mice, as with virus passaged in cell culture, were not under strong selection by HIV-1-specific antibodies and that these mutations may otherwise confer a selective advantage for an Env function possibly involving increased CD4 binding affinity, CD4 independence, or more rapid fusion (38, 48, 64, 66, 77).

In order to determine if increased neutralization sensitivity was linked to CD4 binding affinity, clones were selected that represented a range of sensitivities to the anti-V3 antibody, from relatively resistant to highly sensitive. Sensitivity to competitive inhibition by an anti-CD4 antibody, Leu3a, was used to evaluate CD4 binding efficiency. Table 2 shows the relative sensitivities of viruses pseudotyped with selected Env proteins to inhibition of entry by Leu3a. Env proteins that were highly sensitive to the anti-V3 antibody, those derived from mouse 6, showed a small but significant decrease in sensitivity to Leu3a, while the JRCSF I165K and D167N mutants, which exhibited intermediate sensitivities to the anti-V3 antibody, exhibited only a marginal decrease in Leu3a sensitivity. This indicates that these Env proteins have enhanced CD4 binding. When viral fusion kinetics were measured in a time-of-addition experiment using T20, we failed to measure an increase in the rate of entry for any of these clones (data not shown). Although the mutations at positions 165 and 167 conferred only a slight increase in CD4 binding affinity, indicating that other mutations are likely involved in conferring a stronger phenotype, they are linked to anti-V3 antibody sensitivity and likely contribute to a more open Env conformation that potentiates CD4 binding and an increase in replication capacity. This is con-

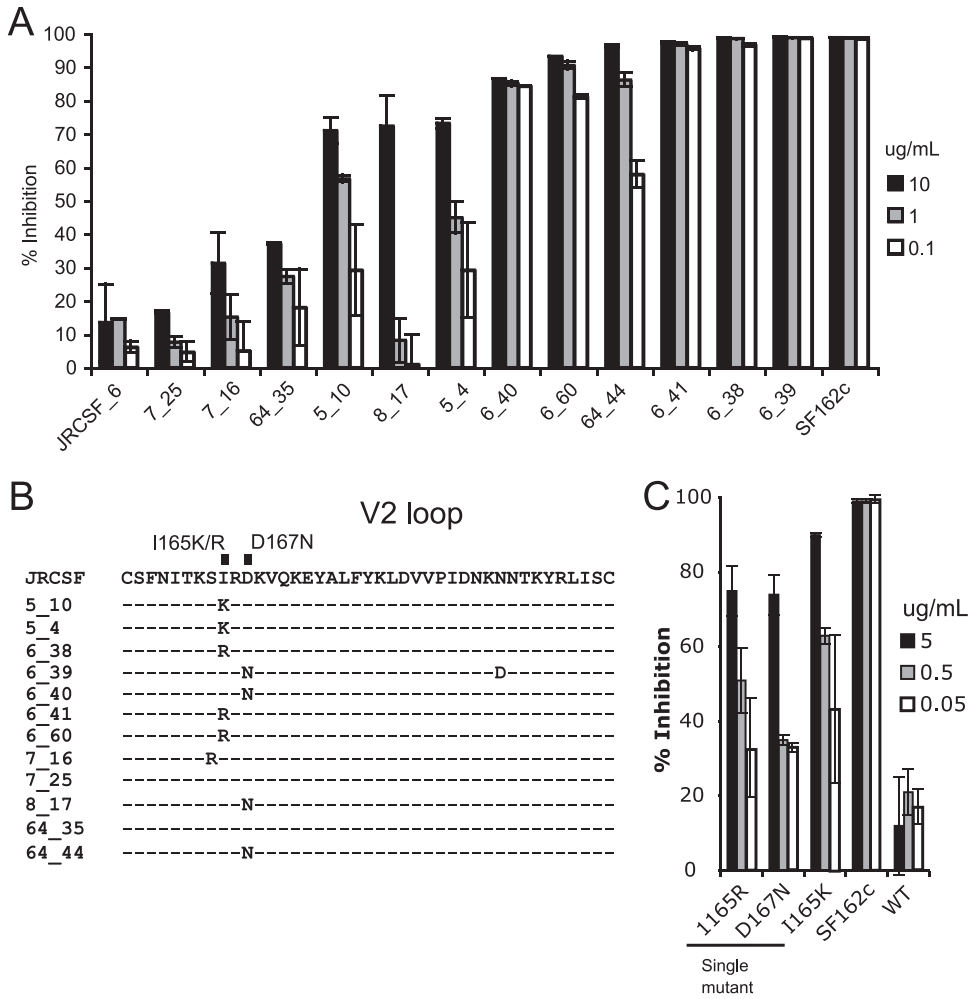

FIG. 5. Neutralization sensitivities of selected envelope clones and mutants to 447-52D. (A) Clone names give the mouse number followed by the clone number (e.g., 5_10). Percent inhibition is indicated for 447-52D antibody concentrations of 10 to 0.1 μg/ml. Error bars represent the ranges for two replicates. SF162c, a neutralization-sensitive chimeric *env* gene in which the V3 region of HIV-1_{SF162} was replaced with the V3 region from HIV-1_{JRFL} (71). (B) Alignment of the V2 loops of clones tested for neutralization sensitivity to 447-52D. Positions 165 and 167 are indicated. (C) Neutralization sensitivity of HIV-1_{JRCSF} with I165R, D167N, or I165K substitution alone.

TABLE 2. Resistance to anti-CD4 antibody inhibition

Clone[a]	IC_{50}	
	Leu3a (mean [95% CI]) (ng/ml)[b]	447-52D (μg/ml)[c]
6_38	40.9 (34.7–48.2)	<0.1
6_39	43.2 (39.3–47.6)	<0.1
JRCSF I165K	35.3 (31.0–40.2)	0.2
JRCSF D167N	33.0 (29.4–37.1)	1.4
7_16	23.2 (19.3–27.7)	>10
7_25	23.0 (19.6–27.1)	>10
JRCSF	23.5 (19.8–28.0)	>10

[a] The first position in the clone name indicates the mouse number or the parental clone (for mutants).

[b] Fifty percent inhibitory concentration (IC_{50}) values were obtained from a sigmoidal dose-response curve fitted to 8 to 10 concentration data points (3 replicates per data point) ranging from 2 to 10^{-4} μg/ml.

[c] IC_{50} values were obtained from a linear curve fitted to 3 concentration data points, 10, 1, and 0.1 μg/ml.

sistent with the observation that Envs with these mutations become fixed in multiple mouse viral populations.

When linkage analysis was performed, two sets of mutations were found to be in high linkage disequilibrium with each other in multiple mouse viral populations. Substitutions at positions 165 and 167 exhibited mutual exclusivity in the two mice in which both substitutions were present (mice 5 and 6), and each was linked to a different position in the same PNLG sequon, occupying positions 411 to 413. In mouse 6, substitutions at positions 165 and 167 were linked to PNLG site-disrupting substitutions at positions 413 and 411, respectively ($P < 0.0001$ for both). In mouse 5, changes at positions 165 and 413 were also strongly linked ($P < 0.001$), although linkage between positions 167 and 411 was weak. In two other mice (mice 8 and 64), only substitutions at positions 167 and 411 were present, and in mouse 8, they were largely coincident in the subset of genomes where they appeared ($P < 0.01$). In mouse 64, while a substitution at position 167 appeared in 30% of genomes, changes at posi-

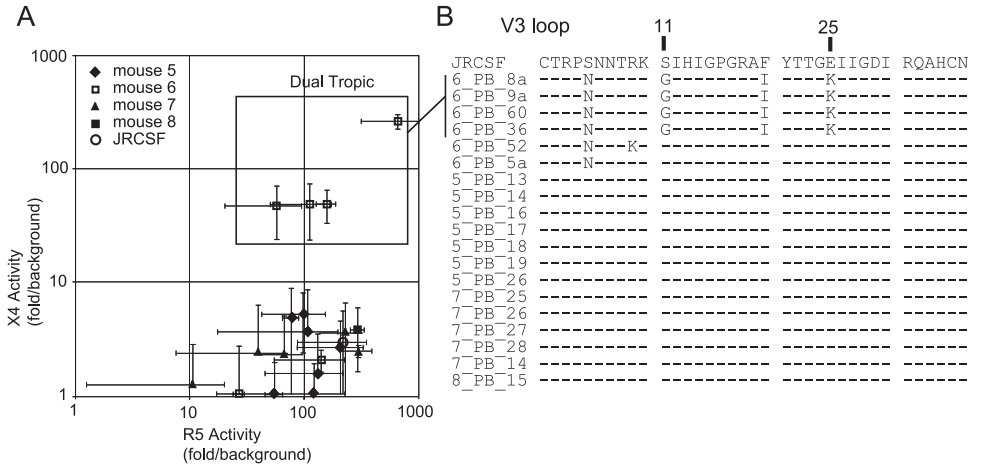

FIG. 6. Phenotypic analysis of coreceptor tropism. (A) Relative CXCR4 and CCR5 activities of *env* clones from four mice at week 44 postinfection in a pseudotype entry assay using U87.CD4 cells expressing either CXCR4 or CCR5. *env* clones exhibiting X4 usage are boxed and labeled "dual tropic." Error bars represent the standard deviations for three replicates. These data are representative of multiple tropism assays. (B) Alignment of the V3 loops of *env* clones tested for panel A. Clone names indicate the mouse number, tissue origin (peripheral blood [PB]), and clone number. Env proteins exhibiting X4 tropism, boxed in panel A and indicated as "dual tropic," are indicated in the alignment as those with changes in their V3 loops at positions 11 and 25 associated with the ability to use CXCR4. These variants were identified only in mouse 6 and comprised 15% of the population.

tion 411 appeared in all genomes. Weak linkage between positions in V3 and either position in the 411 sequon were also observed in mice 6 and 8. In summary, the substitutions at positions 165 and 167, themselves implicated in alterations of envelope structure, showed linkage to mutations that disrupted the same distant PNLG site, but the linkage was to different positions within the PNLG sequon. It seems likely that the specific amino acid that removes the carbohydrate attachment at position 411 has a context-dependent effect based on the substitution at position 165 or 167.

Evolution of coreceptor usage. HIV-1 infection is primarily established by variants that utilize CCR5 as their coreceptor for entry into target cells (R5 viruses), but in about half of subtype B chronic infections, viral variants emerge that can use CXCR4 as their coreceptor (termed X4 viruses) (19, 49). The sequence of the V3 loop is a strong genetic determinant of, and can be used to predict, HIV-1 coreceptor phenotype (26, 41, 68). Because HIV-1_{JRCSF} utilizes CCR5 exclusively, we were interested in determining if this virus had evolved to use CXCR4 in any of these animals. Six of 39 (15%) sequences from mouse 6 exhibited an X4-associated genotype, with amino acid substitutions S11G and E25K in V3 (Fig. 6B), at sites where variability is linked to coreceptor switching (63). In addition, nearly all V3 sequences from mouse 6 (92%) also had an S5N substitution, which represented a reversion to the subtype B consensus (Fig. 6B). A serine at this position has been linked to CCR5 usage (63), indicating that this reversion may be linked to evolution of an X4 phenotype. These and additional selected clones from mice 5 to 8 were tested for the ability to enter indicator cell lines expressing CD4 and either CXCR4 or CCR5. Consistent with their sequence prediction, the clones from mouse 6 that exhibited the genetic features of X4 usage were able to infect a $CD4^+$ $CXCR4^+$ indicator cell line and were therefore classified as having an X4 phenotype (Fig. 6A and B). Reintroduction of the X4-associated V3 sequence into the original HIV-1_{JRCSF} *env* gene was sufficient to confer CXCR4 tropism in the entry assay (data not shown). X4 variants emerged in the peripheral blood late in infection; they were not detected at week 40 (0 of 29 sequences) but were detected at week 43 in 3 of 13 sequences (23%). Thus, HIV-1 has the potential to evolve to use CXCR4 in this model, following an evolutionary path similar to what is observed in natural infections.

Compartmentalization of phenotypic variants. HIV-1 can be found in multiple tissue compartments in the course of a human infection, which in some cases leads to the establishment of isolated or compartmentalized viral populations (98). We were therefore interested in investigating whether or not variants were compartmentalized in different tissue compartments in the mouse. Mouse 6 in particular, which harbored an X4 virus population, provided the opportunity to examine the tissue distribution of variants with distinct coreceptor phenotypes. Viral *env* genes (V1 to V5) from this mouse were successfully amplified and sequenced from DNAs extracted from the spleen (SP), bone marrow (BM), and mesenteric lymphoid tissue (MLN), using the same limiting-dilution technique employed for plasma RNA. Attempts to amplify viral DNA from the thymus were unsuccessful. Phylogenetic analysis of sequences recovered from these three tissues, together with sequences from peripheral blood plasma, revealed the distinct clustering of X4 viruses within the tree, which was suggestive of clonal outgrowth of the X4 variant (Fig. 7). In addition, X4-like variants comprised 95% of variants identified in the MLN, indicating compartmentalization of this phenotype in this tissue ($P < 0.0001$). Phenotypic testing of a sample of variants with X4-like V3 sequences from the MLN confirmed their X4 phenotype (data not shown). Variants recovered from the spleen were phylogenetically intermingled with those from the peripheral blood and exhibited the same distribution. With these limited data, we cannot determine if X4 compartmentalization in the MLN is due to stochastic seeding of or initial evolution in this tissue site or if X4 viruses have a selective advantage in the MLN in this model. However, these data do

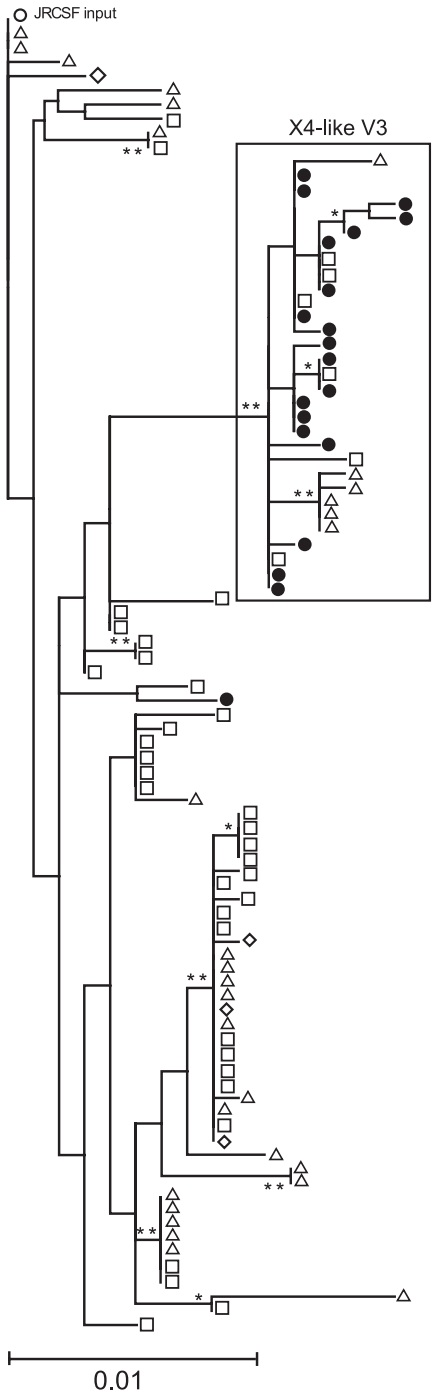

FIG. 7. Maximum likelihood phylogeny of *env* variants (V1 to C5) recovered from different tissue compartments in mouse 6. Bootstrap values of >80% and >50% are indicated by double and single asterisks at nodes, respectively. Sequences were derived from viral DNA except in the case of sequences from the peripheral blood, which were from plasma viral RNA. The tissues of origin of sequences are indicated by symbols. Triangles, spleen; diamonds, bone marrow; squares, peripheral blood; closed circles, mesenteric lymph node. An open circle indicates the JRCSF input sequence. The boxed cluster indicates X4-like V3 sequences, which contain substitutions at positions 11 and 25, in addition to others, and cluster together. A subset of these sequences was phenotypically tested to confirm tropism. Of the variants in the MLN, 95% contained an X4-like V3 sequence, indicating compartmentalization of this phenotype in this tissue in mouse 6 ($P < 0.0001$).

demonstrate the potential for subpopulations of virus to disseminate, evolve, and replicate independently in different tissues.

Genetic compartmentalization between the MLN and PB was assessed in mice 7, 8, and 64. Viral DNA was not successfully amplified from other mice or other tissues. In mice 7 and 8, sequences were well equilibrated between the PB plasma RNA and MLN tissue DNA. In mouse 64, a single synonymous mutation was enriched in the MLN ($P = 0.0001$; Fisher's exact test), providing a second example of compartmentalization, although the overall genetic divergence between the two compartments was small (data not shown) and likely not based on phenotypic differences, at least within the Env protein.

DISCUSSION

Current models being used to study various aspects of HIV-1 infection include the genetically immunodeficient Rag2$^{-/-}$ $\gamma_C{}^{-/-}$ mouse reconstituted with a human immune system by transplantation of human hematopoietic stem cells (DKO-hu-HSC mouse) (1, 3, 6, 30, 102). However, a detailed analysis of viral diversification and evolution in long-term infections has not been carried out with this system. In this study, we examined the viral populations of DKO-hu-HSC mice with sustained infection for up to 44 weeks. We found that HIV-1 diversifies at nearly the same rate as that observed in human infections. We observed evolution of CXCR4 coreceptor use, a characteristic of many natural chronic infections. In addition, we detected evolution toward increased sensitivity to a conformation-dependent V3 neutralizing antibody, increased CD4 binding affinity, and a general loss of N-linked glycosylation sites.

Acute HIV-1 infection in humans is marked by high levels of viral replication. Within several weeks after infection, the cytotoxic T-lymphocyte (CTL) response appears and leads to suppression of peak viremia (12, 76). Following this initial immune response, variants emerge that have escaped CTL detection, marking the beginning of continuing evolution of HIV-1 in response to this selective pressure (12, 77). Between 4 and 5 weeks postinfection (typically), HIV-1-specific antibodies appear (seroconversion), with some antibodies directed against the Env protein that can potentially select for neutralization escape variants (25, 27, 91). Selection of immune escape variants results in increasing viral diversity, which begins after seroconversion and continues into the chronic stage of infection, although the tempo of immune escape is highly variable and depends on the strength of the immune response and the extent of immune dysregulation (27). Thus, the increasing variability in the *env* gene observed in human infection after seroconversion has a large component that is attributable to escape from immune pressure. In contrast, the DKO-hu-HSC model appears to lack a robust adaptive immune response to HIV-1 (1, 3, 30, 102). However, we observed similar rates of divergence and degrees of diversity in comparing viral populations from infected human subjects and DKO-hu-HSC mice. One interpretation is that the rates of divergence in DKO-hu-HSC mouse and human infections, while similar, are driven by different selective pressures acting on the population. For example, the virus may be evolving either in response to constant immune pressure or as a result of selection for more efficient Env function in the absence of immune selection, as has been observed in cell culture (38, 48, 64, 65,

77), or perhaps also in the late stage of infection associated with immunodeficiency. The emergence of the same amino acid substitutions in multiple mice, particularly those that were linked to a phenotype such as enhanced CD4 binding or loss of glycosylation sites, was interpreted as evidence of positive selection. Analysis of selection based on the relative rates of synonymous (dS) and nonsynonymous (dN) mutations across the V1-to-C5 region revealed no consistent pattern. However, this type of analysis is compromised when too few synonymous or nonsynonymous mutations have accumulated to lend enough power to the analysis or if only a few sites are under strong positive or negative selection. For this model and over this period, the per-codon dN/dS rate ratio could not be determined reliably because of a lack of mutations at synonymous sites.

Some of the patterns of mutations were also similar to those observed in humans, with most substitutions concentrated in the variable loops and with the detection of G-to-A hypermutations. However, evolution in this model is distinguished from natural infection by the quality of some mutations that grew out in the population. We observed that a number of Env variants isolated from several mice exhibited increased sensitivity to V3-specific antibodies such as 447-52D, which has been shown to be dependent on Env conformation and generally inactive against primary isolates, presumably as a result of occlusion of the V3 epitope in the wild-type, non-receptor-bound conformation of Env (7, 48). Specifically, we observed two mutations in V2 that were selected in most mice and resulted in amino acid substitutions I165R and D167N. We found that all of the viruses tested that evolved neutralization sensitivity to 447-52D had one of these two substitutions and that either of these alone, when reintroduced into the parental virus, HIV-1_{JRCSF}, rendered the virus more sensitive to neutralization. Variants with increased anti-V3 antibody sensitivity also exhibited increased resistance to competitive inhibition by the anti-CD4 antibody Leu3a. This was interpreted as an increased CD4 binding efficiency.

Both 165R and 167N substitutions are represented, at approximate frequencies of 3% and 12%, respectively, in the HIV Sequence Database (Los Alamos National Laboratories), whereas the most common amino acids at these positions, I165 and D167, are both found at frequencies of about 67%. These sites therefore exhibit some variability in human infections, and substitutions at these sites, along with other mutations that affect Env conformation, may be markers of a loss of robust humoral immune pressure in late-stage disease, although a direct link has yet to be made for natural infections. These substitutions have, however, been identified in several studies of virus passaged in cell culture (64, 77, 85, 99). While all of these studies found one or both of these substitutions to be linked to increased CD4 binding affinity (or sensitivity to CD4 mimics), the effects that these substitutions have on sensitivity to V3 antibodies in particular vary with the genetic background and the presence of different coevolving substitutions. In our study, the I165R/K and D167N substitutions appear to be mutually exclusive, and their appearance together or in combination with other substitutions may alter their neutralization phenotype. It is likely that these substitutions, along with others observed in viruses that have been passaged in cell culture systems, represent evolution toward heightened Env function through increased CD4 binding affinity or evolution toward CD4 independence, in the absence of neutralizing antibodies, as postulated previously (48, 65, 77). Further studies are required to ascertain whether or not these types of mutations are selected in people during profound immunosuppression and if they are linked to other phenotypes, such as CXCR4 tropism, that appear in late-stage disease.

We also observed an overall loss of specific PNLG sites in multiple mice. Mutations that resulted in the loss of PNLG sites included sites that have been demonstrated to be conserved or selected in a long-term infection in a simian/human immunodeficiency virus model (N339 and N386) (10). Other PNLG sites that were lost have been identified as central in a network of coevolving PNLG sites (N411) (74). The loss of the N386 site, which was observed at a high frequency in three mice, has been implicated in enhancing HIV-1 replication in macrophages, which express low levels of CD4 and likely require changes in Env that increase CD4 affinity in order to be infected efficiently (23). Thus, the observed losses of N-linked glycosylation sites in mice, as with the changes affecting neutralization by V3 antibodies, also might represent selection for changes in Env that increase infectivity in the absence of neutralizing antibodies.

Another feature of natural HIV-1 infection is the emergence, usually late in chronic infection, of variants that use CXCR4 as a coreceptor. This occurs in about 50% of individuals infected with subtype B HIV-1 (19, 49). While this phenotypic switch in the population often coincides with a rapid drop in $CD4^+$ T-cell count and with disease progression (19), the selective pressures driving this switch are not clear. A stochastic model where the appearance of X4 variants is limited by the chance occurrence of the right combination of mutations does not explain their emergence in humans, where the host likely also has to be immunodeficient (32, 36, 49). In one infected DKO-hu-HSC mouse, we detected variants that could use CXCR4 as their coreceptor in addition to CCR5. These variants had distinct V3 sequences that were indicative of CXCR4 usage and were detected at weeks 43 and 44 but not at week 40. Coincidentally, 3 days prior to the detection of X4 variants, Ontak treatment (see Materials and Methods) was administered, which resulted in Treg cell depletion and increased T-cell activation. Ontak treatment may therefore have played a role in creating an environment that potentiated X4 virus emergence in the periphery. However, it is also likely that the X4 variant preexisted in the MLN, the tissue in which it was found to be compartmentalized 1 week later. Only one of three mice treated with Ontak developed detectable X4 virus, and no other biological characteristic of the virus examined in this study could be attributed to an Ontak treatment effect. Early steps in the evolution of CXCR4 tropism may require the same conformational changes that render the virus sensitive to specific antibodies (14). A small effective population size in these mice compared to that in humans could also partly explain the emergence and outgrowth of X4 variants following a stochastic process (13, 79). Nonetheless, this animal model provides the opportunity to explore further the link between X4 emergence and other Env phenotypes that evolve in the absence of a robust immune response.

Examination of the tissue distribution of variants in the mouse in which the X4 virus emerged showed that 95% of variants in the MLN were X4 viruses, compared to 15% in the

peripheral blood and 22% in the spleen. While it is possible that apparent compartmentalization of X4 variants in the MLN was a result of chance seeding, there may also be a selective advantage for X4 viruses in this compartment. Previous studies have identified the thymus as a likely environment for X4 virus selection due to the high levels of CXCR4 expressed on resident T cells (82). In contrast, the MLN in wild-type mice is responsible for linking both inductive and effector sites of the gut-associated lymphoid tissue (GALT), such as Peyer's patches, the lamina propria, and mucosal epithelium. As such, MLNs normally harbor a large population of activated T cells, predominantly with a memory phenotype, expressing high levels of CCR5. It is the large number of activated $CD4^+$ $CCR5^+$ T cells found in the GALT that are thought to support establishment and high levels of replication of the CCR5-tropic viruses responsible for initial infection. Indeed, this tissue is decimated during peak viremia in the acute stage of infection (31, 56). Thus, it is unclear how CXCR4-tropic viruses would have an advantage in this environment under normal conditions. However, the MLN in this model, which is populated by human T cells, may represent a different environment than that seen in healthy humans or wild-type mice. The GALT has been shown to be underdeveloped in this model (37), indicating that the MLN may not be populated by the same $CD4^+$ T-cell subsets present in this tissue in a normal individual. Further exploration is required to assess more fully the cellular subsets populating this and other compartments in this model and the effects that they have on the selection of viruses with different phenotypes.

ACKNOWLEDGMENTS

We thank the Los Alamos National Laboratories HIV Database group for helpful discussions and for the development of a vast array of user-friendly online tools for genetic analysis. We also thank Rachel Lovingood and Tom Denny of the CHAVI for Western blot analysis of the mouse samples.

This work was supported by NIH grant R37-AI44667 to R.S. and grant R01-AI077454 to L.S. W.L.I. was supported in part by NIH training grant T32-AI07419. This work was also supported by the UNC Center for AIDS Research (NIH award P30-AI50410) and the Lineberger Comprehensive Cancer Center (NIH award P30-CA16086).

REFERENCES

1. **An, D. S., B. Poon, R. H. T. Fang, K. Weijer, B. Blom, H. Spits, I. S. Chen, and C. H. Uittenbogaart.** 2007. Use of a novel chimeric mouse model with a functionally active human immune system to study human immunodeficiency virus type 1 infection. Clin. Vaccine Immunol. **14:**391–396.
2. **Baba, M., O. Nishimura, N. Kanzaki, M. Okamoto, H. Sawada, Y. Iizawa, M. Shiraishi, Y. Aramaki, K. Okonogi, Y. Ogawa, K. Meguro, and M. Fujino.** 1999. A small-molecule, nonpeptide CCR5 antagonist with highly potent and selective anti-HIV-1 activity. Proc. Natl. Acad. Sci. USA **96:** 5698–5703.
3. **Baenziger, S., R. Tussiwand, E. Schlaepfer, L. Mazzucchelli, M. Heikenwalder, M. O. Kurrer, S. Behnke, J. Frey, A. Oxenius, H. Joller, A. Aguzzi, M. G. Manz, and R. F. Speck.** 2006. Disseminated and sustained HIV infection in CD34+ cord blood cell-transplanted Rag2−/−gamma c−/− mice. Proc. Natl. Acad. Sci. USA **103:**15951–15956.
4. **Beaumont, T., E. Quakkelaar, A. van Nuenen, R. Pantophlet, and H. Schuitemaker.** 2004. Increased sensitivity to CD4 binding site-directed neutralization following in vitro propagation on primary lymphocytes of a neutralization-resistant human immunodeficiency virus IIIB strain isolated from an accidentally infected laboratory worker. J. Virol. **78:**5651–5657.
5. **Berges, B. K., S. R. Akkina, J. M. Folkvord, E. Connick, and R. Akkina.** 2008. Mucosal transmission of R5 and X4 tropic HIV-1 via vaginal and rectal routes in humanized Rag2−/− gammac−/− (RAG-hu) mice. Virology **373:**342–351.
6. **Berges, B. K., W. H. Wheat, B. E. Palmer, E. Connick, and R. Akkina.** 2006. HIV-1 infection and CD4 T cell depletion in the humanized Rag2−/− gamma c−/− (RAG-hu) mouse model. Retrovirology **3:**76.
7. **Binley, J. M., T. Wrin, B. Korber, M. B. Zwick, M. Wang, C. Chappey, G. Stiegler, R. Kunert, S. Zolla-Pazner, H. Katinger, C. J. Petropoulos, and D. R. Burton.** 2004. Comprehensive cross-clade neutralization analysis of a panel of anti-human immunodeficiency virus type 1 monoclonal antibodies. J. Virol. **78:**13232–13252.
8. **Bjorndal, A., H. Deng, M. Jansson, J. R. Fiore, C. Colognesi, A. Karlsson, J. Albert, G. Scarlatti, D. R. Littman, and E. M. Fenyo.** 1997. Coreceptor usage of primary human immunodeficiency virus type 1 isolates varies according to biological phenotype. J. Virol. **71:**7478–7487.
9. **Blaak, H., A. B. van't Wout, M. Brouwer, B. Hooibrink, E. Hovenkamp, and H. Schuitemaker.** 2000. In vivo HIV-1 infection of CD45RA(+)CD4(+) T cells is established primarily by syncytium-inducing variants and correlates with the rate of CD4(+) T cell decline. Proc. Natl. Acad. Sci. USA **97:** 1269–1274.
10. **Blay, W. M., S. Gnanakaran, B. Foley, N. A. Doria-Rose, B. T. Korber, and N. L. Haigwood.** 2006. Consistent patterns of change during the divergence of human immunodeficiency virus type 1 envelope from that of the inoculated virus in simian/human immunodeficiency virus-infected macaques. J. Virol. **80:**999–1014.
11. **Boots, L. J., P. M. McKenna, B. A. Arnold, P. M. Keller, M. K. Gorny, S. Zolla-Pazner, J. E. Robinson, and A. J. Conley.** 1997. Anti-human immunodeficiency virus type 1 human monoclonal antibodies that bind discontinuous epitopes in the viral glycoproteins can identify mimotopes from recombinant phage peptide display libraries. AIDS Res. Hum. Retrovir. **13:**1549–1559.
12. **Borrow, P., H. Lewicki, X. Wei, M. S. Horwitz, N. Peffer, H. Meyers, J. A. Nelson, J. E. Gairin, B. H. Hahn, M. B. Oldstone, and G. M. Shaw.** 1997. Antiviral pressure exerted by HIV-1-specific cytotoxic T lymphocytes (CTLs) during primary infection demonstrated by rapid selection of CTL escape virus. Nat. Med. **3:**205–211.
13. **Brown, A. J.** 1997. Analysis of HIV-1 env gene sequences reveals evidence for a low effective number in the viral population. Proc. Natl. Acad. Sci. USA **94:**1862–1865.
14. **Bunnik, E. M., E. D. Quakkelaar, A. C. van Nuenen, B. Boeser-Nummink, and H. Schuitemaker.** 2007. Increased neutralization sensitivity of recently emerged CXCR4-using human immunodeficiency virus type 1 strains compared to coexisting CCR5-using variants from the same patient. J. Virol. **81:**525–531.
15. **Chackerian, B., L. M. Rudensey, and J. Overbaugh.** 1997. Specific N-linked and O-linked glycosylation modifications in the envelope V1 domain of simian immunodeficiency virus variants that evolve in the host alter recognition by neutralizing antibodies. J. Virol. **71:**7719–7727.
16. **Choudhary, S. K., N. L. Rezk, W. L. Ince, M. Cheema, L. Zhang, L. Su, R. Swanstrom, A. D. Kashuba, and D. M. Margolis.** 2009. Suppression of HIV-1 viremia with reverse transcriptase and integrase inhibitors, CD4+ T cell recovery, and viral rebound upon therapy interruption in a new model for HIV treatment in humanized Rag2−/− {gamma}c−/− mice. J. Virol. **83:**8254–8258.
17. **Conley, A. J., M. K. Gorny, J. A. Kessler II, L. J. Boots, M. Ossorio-Castro, S. Koenig, D. W. Lineberger, E. A. Emini, C. Williams, and S. Zolla-Pazner.** 1994. Neutralization of primary human immunodeficiency virus type 1 isolates by the broadly reactive anti-V3 monoclonal antibody, 447-52D. J. Virol. **68:**6994–7000.
18. **Connor, R. I., H. Mohri, Y. Cao, and D. D. Ho.** 1993. Increased viral burden and cytopathicity correlate temporally with CD4+ T-lymphocyte decline and clinical progression in human immunodeficiency virus type 1-infected individuals. J. Virol. **67:**1772–1777.
19. **Connor, R. I., K. E. Sheridan, D. Ceradini, S. Choe, and N. R. Landau.** 1997. Change in coreceptor use correlates with disease progression in HIV-1-infected individuals. J. Exp. Med. **185:**621–628.
20. **Delwart, E. L., J. I. Mullins, P. Gupta, G. H. Learn, Jr., M. Holodniy, D. Katzenstein, B. D. Walker, and M. K. Singh.** 1998. Human immunodeficiency virus type 1 populations in blood and semen. J. Virol. **72:**617–623.
21. **Denton, P. W., J. D. Estes, Z. Sun, F. A. Othieno, B. L. Wei, A. K. Wege, D. A. Powell, D. Payne, A. T. Haase, and J. V. Garcia.** 2008. Antiretroviral pre-exposure prophylaxis prevents vaginal transmission of HIV-1 in humanized BLT mice. PLoS Med. **5:**e16.
22. **Denton, P. W., and J. V. Garcia.** 2009. Novel humanized murine models for HIV research. Curr. HIV/AIDS Rep. **6:**13–19.
23. **Dunfee, R. L., E. R. Thomas, J. Wang, K. Kunstman, S. M. Wolinsky, and D. Gabuzda.** 2007. Loss of the N-linked glycosylation site at position 386 in the HIV envelope V4 region enhances macrophage tropism and is associated with dementia. Virology **367:**222–234.
24. **Edmonson, P. F., and J. I. Mullins.** 1992. Efficient amplification of HIV half-genomes from tissue DNA. Nucleic Acids Res. **20:**4933.
25. **Fiebig, E. W., D. J. Wright, B. D. Rawal, P. E. Garrett, R. T. Schumacher, L. Peddada, C. Heldebrant, R. Smith, A. Conrad, S. H. Kleinman, and M. P. Busch.** 2003. Dynamics of HIV viremia and antibody seroconversion in plasma donors: implications for diagnosis and staging of primary HIV infection. AIDS **17:**1871–1879.
26. **Fouchier, R. A., M. Groenink, N. A. Kootstra, M. Tersmette, H. G. Huisman, F. Miedema, and H. Schuitemaker.** 1992. Phenotype-associated se-

quence variation in the third variable domain of the human immunodeficiency virus type 1 gp120 molecule. J. Virol. **66:**3183–3187.
27. **Frost, S. D., T. Wrin, D. M. Smith, S. L. Kosakovsky Pond, Y. Liu, E. Paxinos, C. Chappey, J. Galovich, J. Beauchaine, C. J. Petropoulos, S. J. Little, and D. D. Richman.** 2005. Neutralizing antibody responses drive the evolution of human immunodeficiency virus type 1 envelope during recent HIV infection. Proc. Natl. Acad. Sci. USA **102:**18514–18519.
28. **Fulcher, J. A., Y. Hwangbo, R. Zioni, D. Nickle, X. Lin, L. Heath, J. I. Mullins, L. Corey, and T. Zhu.** 2004. Compartmentalization of human immunodeficiency virus type 1 between blood monocytes and CD4+ T cells during infection. J. Virol. **78:**7883–7893.
29. **Gavel, Y., and G. von Heijne.** 1990. Sequence differences between glycosylated and non-glycosylated Asn-X-Thr/Ser acceptor sites: implications for protein engineering. Protein Eng. **3:**433–442.
30. **Gorantla, S., H. Sneller, L. Walters, J. G. Sharp, S. J. Pirruccello, J. T. West, C. Wood, S. Dewhurst, H. E. Gendelman, and L. Poluektova.** 2007. Human immunodeficiency virus type 1 pathobiology studied in humanized BALB/c-Rag2−/− gamma c−/− mice. J. Virol. **81:**2700–2712.
31. **Guadalupe, M., E. Reay, S. Sankaran, T. Prindiville, J. Flamm, A. McNeil, and S. Dandekar.** 2003. Severe CD4+ T-cell depletion in gut lymphoid tissue during primary human immunodeficiency virus type 1 infection and substantial delay in restoration following highly active antiretroviral therapy. J. Virol. **77:**11708–11717.
32. **Harouse, J. M., C. Buckner, A. Gettie, R. Fuller, R. Bohm, J. Blanchard, and C. Cheng-Mayer.** 2003. CD8+ T cell-mediated CXC chemokine receptor 4-simian/human immunodeficiency virus suppression in dually infected rhesus macaques. Proc. Natl. Acad. Sci. USA **100:**10977–10982.
33. **Harrington, P. R., M. J. Connell, R. B. Meeker, P. R. Johnson, and R. Swanstrom.** 2007. Dynamics of simian immunodeficiency virus populations in blood and cerebrospinal fluid over the full course of infection. J. Infect. Dis. **196:**1058–1067.
34. **He, J., S. Choe, R. Walker, P. Di Marzio, D. O. Morgan, and N. R. Landau.** 1995. Human immunodeficiency virus type 1 viral protein R (Vpr) arrests cells in the G2 phase of the cell cycle by inhibiting p34cdc2 activity. J. Virol. **69:**6705–6711.
35. **Hendrix, C. W., C. Flexner, R. T. MacFarland, C. Giandomenico, E. J. Fuchs, E. Redpath, G. Bridger, and G. W. Henson.** 2000. Pharmacokinetics and safety of AMD-3100, a novel antagonist of the CXCR-4 chemokine receptor, in human volunteers. Antimicrob. Agents Chemother. **44:**1667–1673.
36. **Ho, S. H., S. Tasca, L. Shek, A. Li, A. Gettie, J. Blanchard, D. Boden, and C. Cheng-Mayer.** 2007. Coreceptor switch in R5-tropic simian/human immunodeficiency virus-infected macaques. J. Virol. **81:**8621–8633.
37. **Hofer, U., S. Baenziger, M. Heikenwalder, E. Schlaepfer, N. Gehre, S. Regenass, T. Brunner, and R. F. Speck.** 2008. RAG2−/− gamma (c)−/− mice transplanted with CD34+ cells from human cord blood show low levels of intestinal engraftment and are resistant to rectal transmission of human immunodeficiency virus. J. Virol. **82:**12145–12153.
38. **Hoffman, T. L., C. C. LaBranche, W. Zhang, G. Canziani, J. Robinson, I. Chaiken, J. A. Hoxie, and R. W. Doms.** 1999. Stable exposure of the coreceptor-binding site in a CD4-independent HIV-1 envelope protein. Proc. Natl. Acad. Sci. USA **96:**6359–6364.
39. **Ince, W. L., P. R. Harrington, G. L. Schnell, M. Patel-Chhabra, C. L. Burch, P. Menezes, R. W. Price, J. J. Eron, Jr., and R. I. Swanstrom.** 2009. Major coexisting human immunodeficiency virus type 1 env gene subpopulations in the peripheral blood are produced by cells with similar turnover rates and show little evidence of genetic compartmentalization. J. Virol. **83:**4068–4080.
40. **Ishikawa, F., M. Yasukawa, B. Lyons, S. Yoshida, T. Miyamoto, G. Yoshimoto, T. Watanabe, K. Akashi, L. D. Shultz, and M. Harada.** 2005. Development of functional human blood and immune systems in NOD/SCID/IL2 receptor {gamma} chain(null) mice. Blood **106:**1565–1573.
41. **Jensen, M. A., F. S. Li, A. B. van't Wout, D. C. Nickle, D. Shriner, H. X. He, S. McLaughlin, R. Shankarappa, J. B. Margolick, and J. I. Mullins.** 2003. Improved coreceptor usage prediction and genotypic monitoring of R5-to-X4 transition by motif analysis of human immunodeficiency virus type 1 env V3 loop sequences. J. Virol. **77:**13376–13388.
42. **Jern, P., R. A. Russell, V. K. Pathak, and J. M. Coffin.** 2009. Likely role of APOBEC3G-mediated G-to-A mutations in HIV-1 evolution and drug resistance. PLoS Pathog. **5:**e1000367.
43. **Jiang, Q., L. Zhang, R. Wang, J. Jeffrey, M. L. Washburn, D. Brouwer, S. Barbour, G. I. Kovalev, D. Unutmaz, and L. Su.** 2008. FoxP3+CD4+ regulatory T cells play an important role in acute HIV-1 infection in humanized Rag2−/−gammaC−/− mice in vivo. Blood **112:**2858–2868.
44. **Katoh, K., and H. Toh.** 2008. Recent developments in the MAFFT multiple sequence alignment program. Brief. Bioinform. **9:**286–298.
45. **Keele, B. F., E. E. Giorgi, J. F. Salazar-Gonzalez, J. M. Decker, K. T. Pham, M. G. Salazar, C. Sun, T. Grayson, S. Wang, H. Li, X. Wei, C. Jiang, J. L. Kirchherr, F. Gao, J. A. Anderson, L. H. Ping, R. Swanstrom, G. D. Tomaras, W. A. Blattner, P. A. Goepfert, J. M. Kilby, M. S. Saag, E. L. Delwart, M. P. Busch, M. S. Cohen, D. C. Montefiori, B. F. Haynes, B. Gaschen, G. S. Athreya, H. Y. Lee, N. Wood, C. Seoighe, A. S. Perelson, T. Bhattacharya, B. T. Korber, B. H. Hahn, and G. M. Shaw.** 2008. Identification and characterization of transmitted and early founder virus envelopes in primary HIV-1 infection. Proc. Natl. Acad. Sci. USA **105:**7552–7557.
46. **Kemal, K. S., B. Foley, H. Burger, K. Anastos, H. Minkoff, C. Kitchen, S. M. Philpott, W. Gao, E. Robison, S. Holman, C. Dehner, S. Beck, W. A. Meyer III, A. Landay, A. Kovacs, J. Bremer, and B. Weiser.** 2003. HIV-1 in genital tract and plasma of women: compartmentalization of viral sequences, coreceptor usage, and glycosylation. Proc. Natl. Acad. Sci. USA **100:**12972–12977.
47. **Koch, M., M. Pancera, P. D. Kwong, P. Kolchinsky, C. Grundner, L. Wang, W. A. Hendrickson, J. Sodroski, and R. Wyatt.** 2003. Structure-based, targeted deglycosylation of HIV-1 gp120 and effects on neutralization sensitivity and antibody recognition. Virology **313:**387–400.
48. **Kolchinsky, P., E. Kiprilov, and J. Sodroski.** 2001. Increased neutralization sensitivity of CD4-independent human immunodeficiency virus variants. J. Virol. **75:**2041–2050.
49. **Koot, M., R. van Leeuwen, R. E. de Goede, I. P. Keet, S. Danner, J. K. Eeftinck Schattenkerk, P. Reiss, M. Tersmette, J. M. Lange, and H. Schuitemaker.** 1999. Conversion rate towards a syncytium-inducing (SI) phenotype during different stages of human immunodeficiency virus type 1 infection and prognostic value of SI phenotype for survival after AIDS diagnosis. J. Infect. Dis. **179:**254–258.
50. **Korber, B.** 2000. HIV signature and sequence variation analysis, p. 55–72. *In* A. G. Rodrigo and G. H. Learn, Jr. (ed.), Computational and evolutionary analysis of HIV molecular sequences. Kluwer Academic Publishers, Dordrecht, The Netherlands.
51. **Korber, B. T., K. J. Kunstman, B. K. Patterson, M. Furtado, M. M. McEvilly, R. Levy, and S. M. Wolinsky.** 1994. Genetic differences between blood- and brain-derived viral sequences from human immunodeficiency virus type 1-infected patients: evidence of conserved elements in the V3 region of the envelope protein of brain-derived sequences. J. Virol. **68:**7467–7481.
52. **Koyanagi, Y., S. Miles, R. T. Mitsuyasu, J. E. Merrill, H. V. Vinters, and I. S. Chen.** 1987. Dual infection of the central nervous system by AIDS viruses with distinct cellular tropisms. Science **236:**819–822.
53. **Kumar, P., H. S. Ban, S. S. Kim, H. Wu, T. Pearson, D. L. Greiner, A. Laouar, J. Yao, V. Haridas, K. Habiro, Y. G. Yang, J. H. Jeong, K. Y. Lee, Y. H. Kim, S. W. Kim, M. Peipp, G. H. Fey, N. Manjunath, L. D. Shultz, S. K. Lee, and P. Shankar.** 2008. T cell-specific siRNA delivery suppresses HIV-1 infection in humanized mice. Cell **134:**577–586.
54. **Kuritzkes, D. R.** 2009. HIV-1 entry inhibitors: an overview. Curr. Opin. HIV AIDS **4:**82–87.
55. **LeMaistre, C. F.** 2000. DAB(389)IL-2 (denileukin diftitox, ONTAK): other potential applications. Clin. Lymphoma **1**(Suppl. 1)**:**S37–S40.
56. **Li, Q., L. Duan, J. D. Estes, Z. M. Ma, T. Rourke, Y. Wang, C. Reilly, J. Carlis, C. J. Miller, and A. T. Haase.** 2005. Peak SIV replication in resting memory CD4+ T cells depletes gut lamina propria CD4+ T cells. Nature **434:**1148–1152.
57. **Li, Y., L. Luo, N. Rasool, and C. Y. Kang.** 1993. Glycosylation is necessary for the correct folding of human immunodeficiency virus gp120 in CD4 binding. J. Virol. **67:**584–588.
58. **Librado, P., and J. Rozas.** 2009. DnaSP v5: a software for comprehensive analysis of DNA polymorphism data. Bioinformatics **25:**1451–1452.
59. **Mangeat, B., P. Turelli, G. Caron, M. Friedli, L. Perrin, and D. Trono.** 2003. Broad antiretroviral defence by human APOBEC3G through lethal editing of nascent reverse transcripts. Nature **424:**99–103.
60. **Manrique, A., P. Rusert, B. Joos, M. Fischer, H. Kuster, C. Leemann, B. Niederost, R. Weber, G. Stiegler, H. Katinger, H. F. Gunthard, and A. Trkola.** 2007. In vivo and in vitro escape from neutralizing antibodies 2G12, 2F5, and 4E10. J. Virol. **81:**8793–8808.
61. **Mbah, H. A., S. Burda, M. K. Gorny, C. Williams, K. Revesz, S. Zolla-Pazner, and P. N. Nyambi.** 2001. Effect of soluble CD4 on exposure of epitopes on primary, intact, native human immunodeficiency virus type 1 virions of different genetic clades. J. Virol. **75:**7785–7788.
62. **Melkus, M. W., J. D. Estes, A. Padgett-Thomas, J. Gatlin, P. W. Denton, F. A. Othieno, A. K. Wege, A. T. Haase, and J. V. Garcia.** 2006. Humanized mice mount specific adaptive and innate immune responses to EBV and TSST-1. Nat. Med. **12:**1316–1322.
63. **Milich, L., B. H. Margolin, and R. Swanstrom.** 1997. Patterns of amino acid variability in NSI-like and SI-like V3 sequences and a linked change in the CD4-binding domain of the HIV-1 Env protein. Virology **239:**108–118.
64. **Mo, H. M., L. Stamatatos, J. E. Ip, C. F. Barbas, P. Parren, D. R. Burton, J. P. Moore, and D. D. Ho.** 1997. Human immunodeficiency virus type 1 mutants that escape neutralization by human monoclonal antibody IgG1b12. J. Virol. **71:**6869–6874.
65. **Moore, J. P., Y. Cao, L. Qing, Q. J. Sattentau, J. Pyati, R. Koduri, J. Robinson, C. F. Barbas III, D. R. Burton, and D. D. Ho.** 1995. Primary isolates of human immunodeficiency virus type 1 are relatively resistant to neutralization by monoclonal antibodies to gp120, and their neutralization is not predicted by studies with monomeric gp120. J. Virol. **69:**101–109.
66. **Moore, J. P., and D. D. Ho.** 1995. HIV-1 neutralization: the consequences

of viral adaptation to growth on transformed T cells. AIDS **9**(Suppl. A)**:** S117–S136.

67. **Nei, M., and T. Gojobori.** 1986. Simple methods for estimating the numbers of synonymous and nonsynonymous nucleotide substitutions. Mol. Biol. Evol. **3:**418–426.
68. **Nelson, J. A., F. Baribaud, T. Edwards, and R. Swanstrom.** 2000. Patterns of changes in human immunodeficiency virus type 1 V3 sequence populations late in infection. J. Virol. **74:**8494–8501.
69. **Ota, T., and M. Nei.** 1994. Variance and covariances of the numbers of synonymous and nonsynonymous substitutions per site. Mol. Biol. Evol. **11:**613–619.
70. **Palmer, S., M. Kearney, F. Maldarelli, E. K. Halvas, C. J. Bixby, H. Bazmi, D. Rock, J. Falloon, R. T. Davey, Jr., R. L. Dewar, J. A. Metcalf, S. Hammer, J. W. Mellors, and J. M. Coffin.** 2005. Multiple, linked human immunodeficiency virus type 1 drug resistance mutations in treatment-experienced patients are missed by standard genotype analysis. J. Clin. Microbiol. **43:** 406–413.
71. **Patel, M. B., N. G. Hoffman, and R. Swanstrom.** 2008. Subtype-specific conformational differences within the V3 region of subtype B and subtype C human immunodeficiency virus type 1 Env proteins. J. Virol. **82:**903–916.
72. **Platt, E. J., K. Wehrly, S. E. Kuhmann, B. Chesebro, and D. Kabat.** 1998. Effects of CCR5 and CD4 cell surface concentrations on infections by macrophagetropic isolates of human immunodeficiency virus type 1. J. Virol. **72:**2855–2864.
73. **Pollakis, G., S. Kang, A. Kliphuis, M. I. Chalaby, J. Goudsmit, and W. A. Paxton.** 2001. N-linked glycosylation of the HIV type-1 gp120 envelope glycoprotein as a major determinant of CCR5 and CXCR4 coreceptor utilization. J. Biol. Chem. **276:**13433–13441.
74. **Poon, A. F., F. I. Lewis, S. L. Pond, and S. D. Frost.** 2007. Evolutionary interactions between N-linked glycosylation sites in the HIV-1 envelope. PLoS Comput. Biol. **3:**e11.
75. **Posada, D., and K. A. Crandall.** 1998. MODELTEST: testing the model of DNA substitution. Bioinformatics **14:**817–818.
76. **Price, D. A., P. J. Goulder, P. Klenerman, A. K. Sewell, P. J. Easterbrook, M. Troop, C. R. Bangham, and R. E. Phillips.** 1997. Positive selection of HIV-1 cytotoxic T lymphocyte escape variants during primary infection. Proc. Natl. Acad. Sci. USA **94:**1890–1895.
77. **Pugach, P., S. E. Kuhmann, J. Taylor, A. J. Marozsan, A. Snyder, T. Ketas, S. M. Wolinsky, B. T. Korber, and J. P. Moore.** 2004. The prolonged culture of human immunodeficiency virus type 1 in primary lymphocytes increases its sensitivity to neutralization by soluble CD4. Virology **321:**8–22.
78. **Rose, P. P., and B. T. Korber.** 2000. Detecting hypermutations in viral sequences with an emphasis on G→A hypermutation. Bioinformatics **16:** 400–401.
79. **Rouzine, I. M., and J. M. Coffin.** 1999. Linkage disequilibrium test implies a large effective population number for HIV in vivo. Proc. Natl. Acad. Sci. USA **96:**10758–10763.
80. **Salazar-Gonzalez, J. F., E. Bailes, K. T. Pham, M. G. Salazar, M. B. Guffey, B. F. Keele, C. A. Derdeyn, P. Farmer, E. Hunter, S. Allen, O. Manigart, J. Mulenga, J. A. Anderson, R. Swanstrom, B. F. Haynes, G. S. Athreya, B. T. Korber, P. M. Sharp, G. M. Shaw, and B. H. Hahn.** 2008. Deciphering human immunodeficiency virus type 1 transmission and early envelope diversification by single-genome amplification and sequencing. J. Virol. **82:**3952–3970.
81. **Salazar-Gonzalez, J. F., M. G. Salazar, B. F. Keele, G. H. Learn, E. E. Giorgi, H. Li, J. M. Decker, S. Wang, J. Baalwa, M. H. Kraus, N. F. Parrish, K. S. Shaw, M. B. Guffey, K. J. Bar, K. L. Davis, C. Ochsenbauer-Jambor, J. C. Kappes, M. S. Saag, M. S. Cohen, J. Mulenga, C. A. Derdeyn, S. Allen, E. Hunter, M. Markowitz, P. Hraber, A. S. Perelson, T. Bhattacharya, B. F. Haynes, B. T. Korber, B. H. Hahn, and G. M. Shaw.** 2009. Genetic identity, biological phenotype, and evolutionary pathways of transmitted/founder viruses in acute and early HIV-1 infection. J. Exp. Med. **206:**1273–1289.
82. **Salemi, M., B. R. Burkhardt, R. R. Gray, G. Ghaffari, J. W. Sleasman, and M. M. Goodenow.** 2007. Phylodynamics of HIV-1 in lymphoid and non-lymphoid tissues reveals a central role for the thymus in emergence of CXCR4-using quasispecies. PLoS One **2:**e950.
83. **Scott, C. F., Jr., S. Silver, A. T. Profy, S. D. Putney, A. Langlois, K. Weinhold, and J. E. Robinson.** 1990. Human monoclonal antibody that recognizes the V3 region of human immunodeficiency virus gp120 and neutralizes the human T-lymphotropic virus type IIIMN strain. Proc. Natl. Acad. Sci. USA **87:**8597–8601.
84. **Shankarappa, R., J. B. Margolick, S. J. Gange, A. G. Rodrigo, D. Upchurch, H. Farzadegan, P. Gupta, C. R. Rinaldo, G. H. Learn, X. He, X. L. Huang, and J. I. Mullins.** 1999. Consistent viral evolutionary changes associated with the progression of human immunodeficiency virus type 1 infection. J. Virol. **73:**10489–10502.
85. **Shibata, J., K. Yoshimura, A. Honda, A. Koito, T. Murakami, and S. Matsushita.** 2007. Impact of V2 mutations on escape from a potent neutralizing anti-V3 monoclonal antibody during in vitro selection of a primary human immunodeficiency virus type 1 isolate. J. Virol. **81:**3757–3768.
86. **Simmonds, P., P. Balfe, C. A. Ludlam, J. O. Bishop, and A. J. Brown.** 1990. Analysis of sequence diversity in hypervariable regions of the external glycoprotein of human immunodeficiency virus type 1. J. Virol. **64:**5840–5850.
87. **Sun, Z., P. W. Denton, J. D. Estes, F. A. Othieno, B. L. Wei, A. K. Wege, M. W. Melkus, A. Padgett-Thomas, M. Zupancic, A. T. Haase, and J. V. Garcia.** 2007. Intrarectal transmission, systemic infection, and CD4+ T cell depletion in humanized mice infected with HIV-1. J. Exp. Med. **204:**705–714.
88. **ter Brake, O., N. Legrand, K. J. von Eije, M. Centlivre, H. Spits, K. Weijer, B. Blom, and B. Berkhout.** 2009. Evaluation of safety and efficacy of RNAi against HIV-1 in the human immune system (Rag-2(−/−)gammac(−/−)) mouse model. Gene Ther. **16:**148–153.
89. **Tersmette, M., R. A. Gruters, F. de Wolf, R. E. de Goede, J. M. Lange, P. T. Schellekens, J. Goudsmit, H. G. Huisman, and F. Miedema.** 1989. Evidence for a role of virulent human immunodeficiency virus (HIV) variants in the pathogenesis of acquired immunodeficiency syndrome: studies on sequential HIV isolates. J. Virol. **63:**2118–2125.
90. **Thomas, E. R., R. L. Dunfee, J. Stanton, D. Bogdan, J. Taylor, K. Kunstman, J. E. Bell, S. M. Wolinsky, and D. Gabuzda.** 2007. Macrophage entry mediated by HIV Envs from brain and lymphoid tissues is determined by the capacity to use low CD4 levels and overall efficiency of fusion. Virology **360:**105–119.
91. **Tomaras, G. D., N. L. Yates, P. Liu, L. Qin, G. G. Fouda, L. L. Chavez, A. C. Decamp, R. J. Parks, V. C. Ashley, J. T. Lucas, M. Cohen, J. Eron, C. B. Hicks, H. X. Liao, S. G. Self, G. Landucci, D. N. Forthal, K. J. Weinhold, B. F. Keele, B. H. Hahn, M. L. Greenberg, L. Morris, S. S. Karim, W. A. Blattner, D. C. Montefiori, G. M. Shaw, A. S. Perelson, and B. F. Haynes.** 2008. Initial B-cell responses to transmitted human immunodeficiency virus type 1: virion-binding immunoglobulin M (IgM) and IgG antibodies followed by plasma anti-gp41 antibodies with ineffective control of initial viremia. J. Virol. **82:**12449–12463.
92. **Traggiai, E., L. Chicha, L. Mazzucchelli, L. Bronz, J. C. Piffaretti, A. Lanzavecchia, and M. G. Manz.** 2004. Development of a human adaptive immune system in cord blood cell-transplanted mice. Science **304:**104–107.
93. **Trkola, A., M. Purtscher, T. Muster, C. Ballaun, A. Buchacher, N. Sullivan, K. Srinivasan, J. Sodroski, J. P. Moore, and H. Katinger.** 1996. Human monoclonal antibody 2G12 defines a distinctive neutralization epitope on the gp120 glycoprotein of human immunodeficiency virus type 1. J. Virol. **70:**1100–1108.
94. **Van Duyne, R., J. Cardenas, R. Easley, W. Wu, K. Kehn-Hall, Z. Klase, S. Mendez, C. Zeng, H. Chen, M. Saifuddin, and F. Kashanchi.** 2008. Effect of transcription peptide inhibitors on HIV-1 replication. Virology **376:**308–322.
95. **Walter, B. L., K. Wehrly, R. Swanstrom, E. Platt, D. Kabat, and B. Chesebro.** 2005. Role of low CD4 levels in the influence of human immunodeficiency virus type 1 envelope V1 and V2 regions on entry and spread in macrophages. J. Virol. **79:**4828–4837.
96. **Watanabe, S., K. Terashima, S. Ohta, S. Horibata, M. Yajima, Y. Shiozawa, M. Z. Dewan, Z. Yu, M. Ito, T. Morio, N. Shimizu, M. Honda, and N. Yamamoto.** 2007. Hematopoietic stem cell-engrafted NOD/SCID/IL2Rgamma null mice develop human lymphoid systems and induce long-lasting HIV-1 infection with specific humoral immune responses. Blood **109:**212–218.
97. **Wei, X., J. M. Decker, S. Wang, H. Hui, J. C. Kappes, X. Wu, J. F. Salazar-Gonzalez, M. G. Salazar, J. M. Kilby, M. S. Saag, N. L. Komarova, M. A. Nowak, B. H. Hahn, P. D. Kwong, and G. M. Shaw.** 2003. Antibody neutralization and escape by HIV-1. Nature **422:**307–312.
98. **Wong, J. K., C. C. Ignacio, F. Torriani, D. Havlir, N. J. Fitch, and D. D. Richman.** 1997. In vivo compartmentalization of human immunodeficiency virus: evidence from the examination of pol sequences from autopsy tissues. J. Virol. **71:**2059–2071.
99. **Wrin, T., T. P. Loh, J. C. Vennari, H. Schuitemaker, and J. H. Nunberg.** 1995. Adaptation to persistent growth in the H9 cell line renders a primary isolate of human immunodeficiency virus type 1 sensitive to neutralization by vaccine sera. J. Virol. **69:**39–48.
100. **Wu, X. L., A. Sambor, M. C. Nason, Z. Y. Yang, L. Wu, S. Zolla-Pazner, G. J. Nabel, and J. R. Mascola.** 2008. Soluble CD4 broadens neutralization of V3-directed monoclonal antibodies and guinea pig vaccine sera against HIV-1 subtype B and C reference viruses. Virology **380:**285–295.
101. **Zhang, H., B. Yang, R. J. Pomerantz, C. Zhang, S. C. Arunachalam, and L. Gao.** 2003. The cytidine deaminase CEM15 induces hypermutation in newly synthesized HIV-1 DNA. Nature **424:**94–98.
102. **Zhang, L., G. I. Kovalev, and L. Su.** 2007. HIV-1 infection and pathogenesis in a novel humanized mouse model. Blood **109:**2978–2981.
103. **Zhang, M., B. Gaschen, W. Blay, B. Foley, N. Haigwood, C. Kuiken, and B. Korber.** 2004. Tracking global patterns of N-linked glycosylation site variation in highly variable viral glycoproteins: HIV, SIV, and HCV envelopes and influenza hemagglutinin. Glycobiology **14:**1229–1246.